

## SUPPORTING INFORMATION

### **Drug encapsulation and release with a nonionic amphiphilic calix[4]pyrrole**

Mana Mirabolghasemi,<sup>a</sup> Necla Bektas,<sup>a</sup> Buse Sancakli,<sup>b</sup> Aydan Dag,<sup>c</sup> and Abdullah Aydogan<sup>\*a</sup>

<sup>a</sup> Department of Chemistry, Istanbul Technical University, 34469 Maslak, Istanbul, Türkiye

<sup>b</sup> Department of Biotechnology, Institute of Health Sciences, Bezmialem Vakif University, Istanbul 34093, Türkiye

<sup>c</sup> Department of Pharmaceutical Chemistry, Faculty of Pharmacy, Bezmialem Vakif University, Istanbul 34093, Türkiye

[aydoganab@itu.edu.tr](mailto:aydoganab@itu.edu.tr)

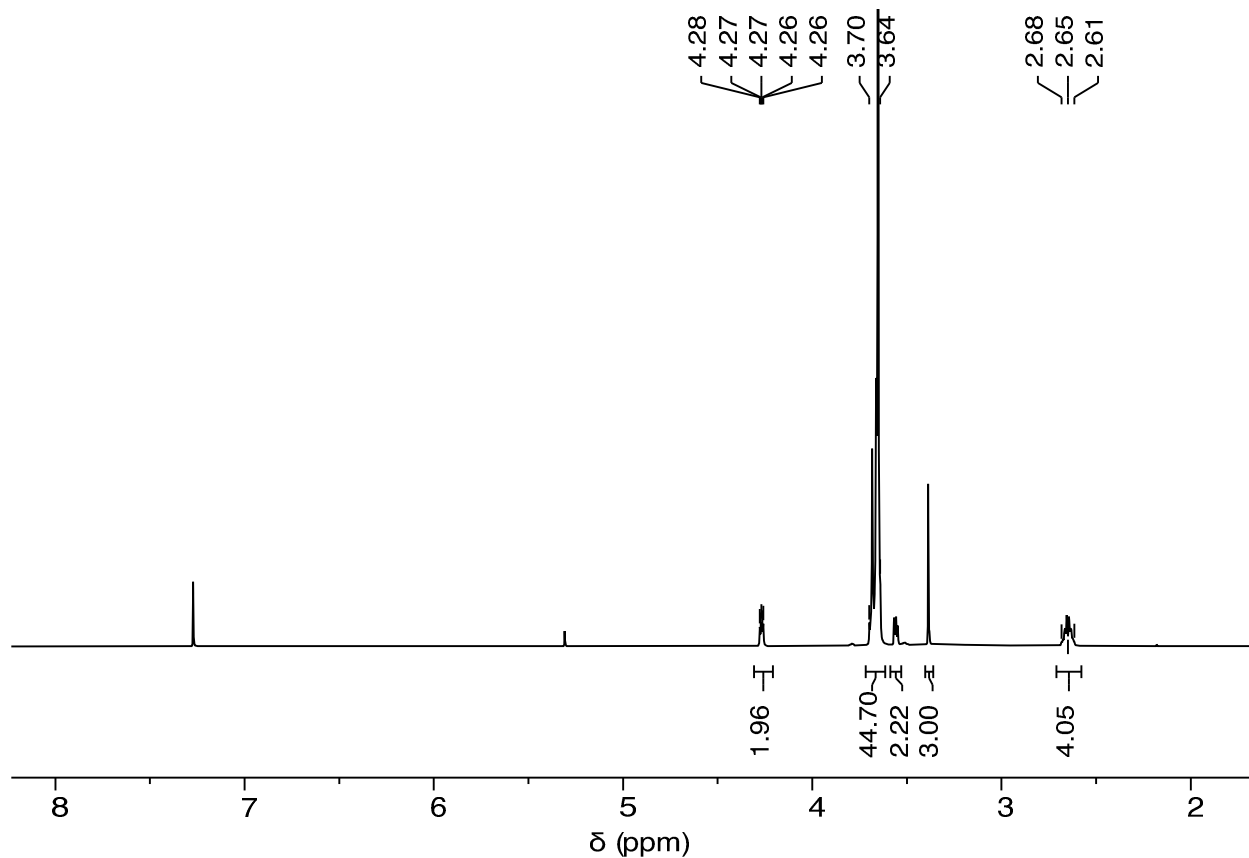


**Fig S1.**  $^1\text{H}$  NMR (500 MHz) spectrum of mPEG-COOH recorded in  $\text{CDCl}_3$ .

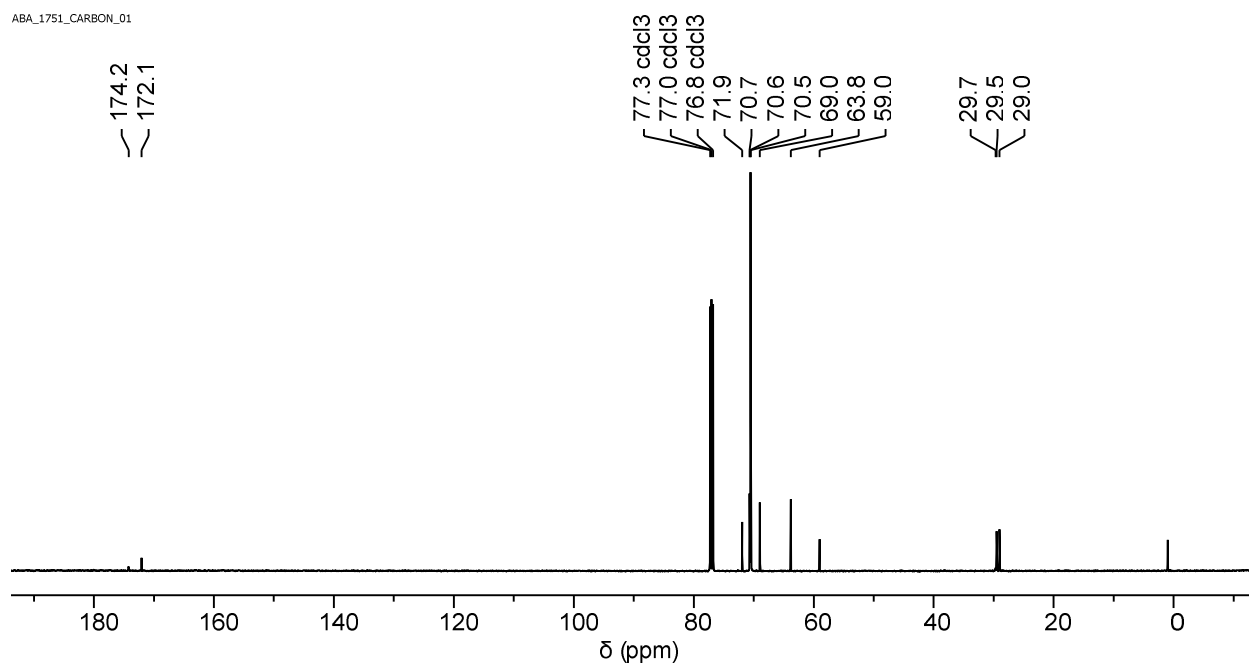


**Fig S2.**  $^{13}\text{C}$  NMR (126 MHz) spectrum of mPEG-COOH recorded in  $\text{CDCl}_3$ .

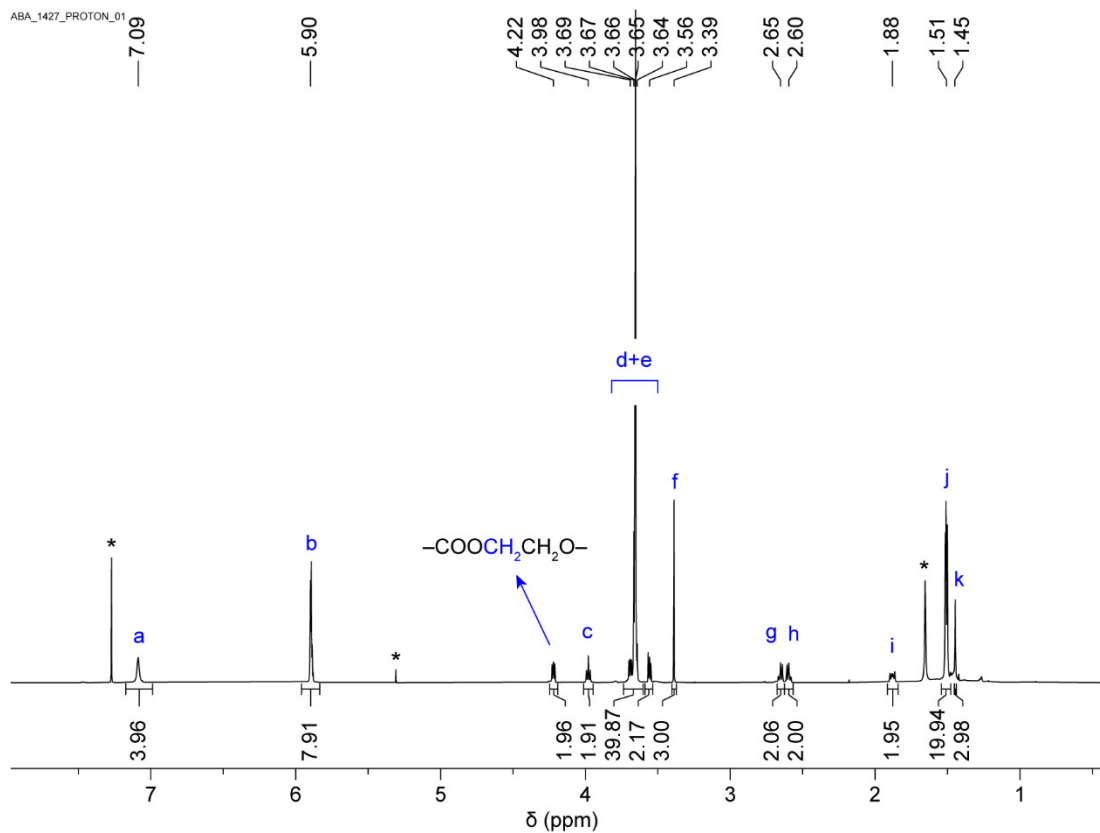


**Fig S3.** <sup>1</sup>H NMR (500 MHz) spectrum of **C4P-PEG** recorded in CDCl<sub>3</sub>.

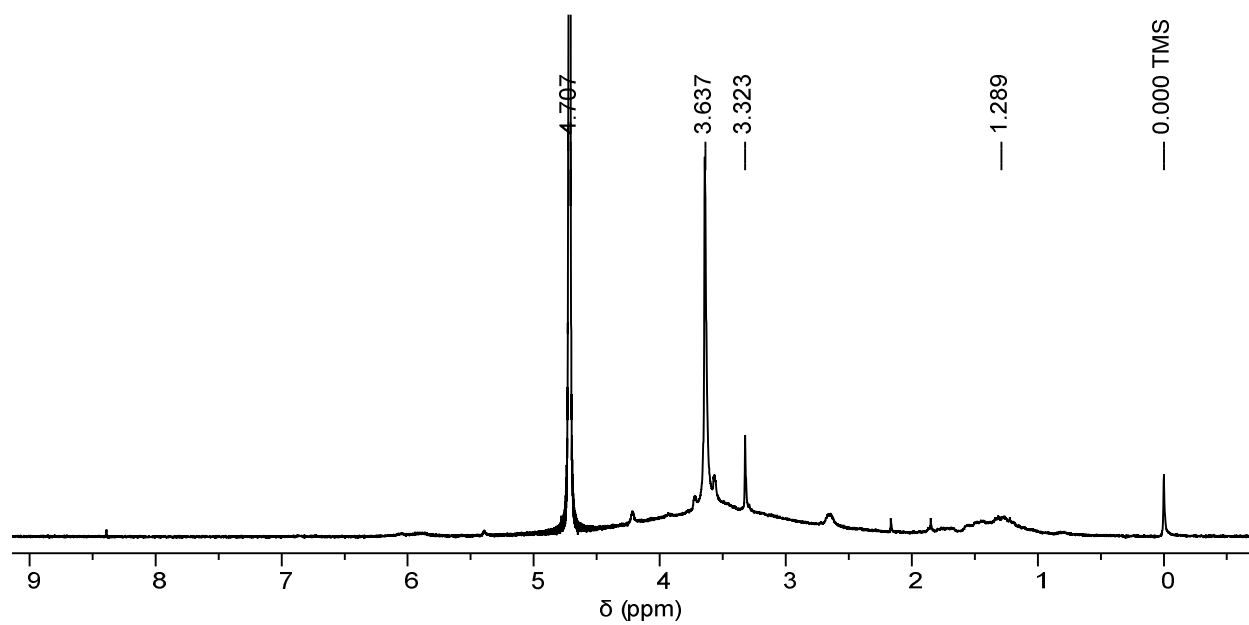


**Fig S4.** <sup>1</sup>H NMR (500 MHz) spectrum of **C4P-PEG** recorded in D<sub>2</sub>O.

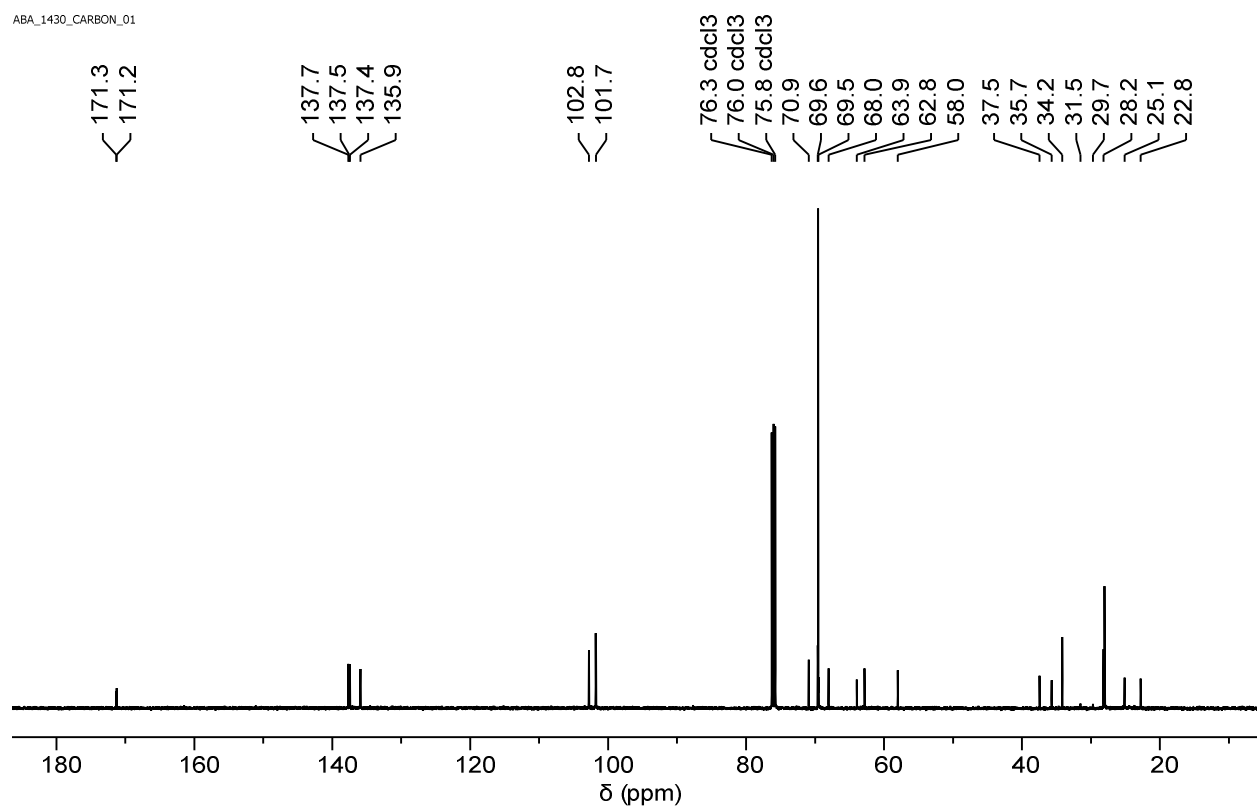


**Fig S5.** <sup>13</sup>C NMR (126 MHz) spectrum of **C4P-PEG** recorded in CDCl<sub>3</sub>.

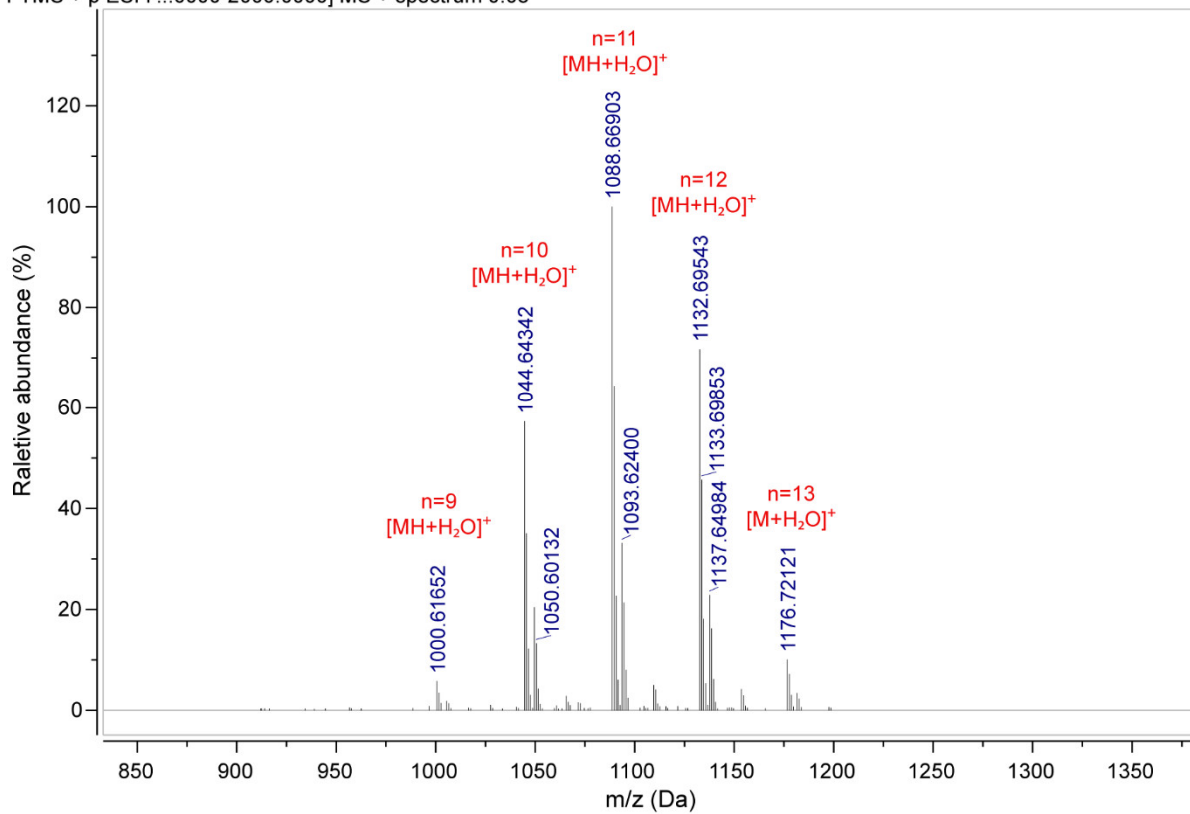
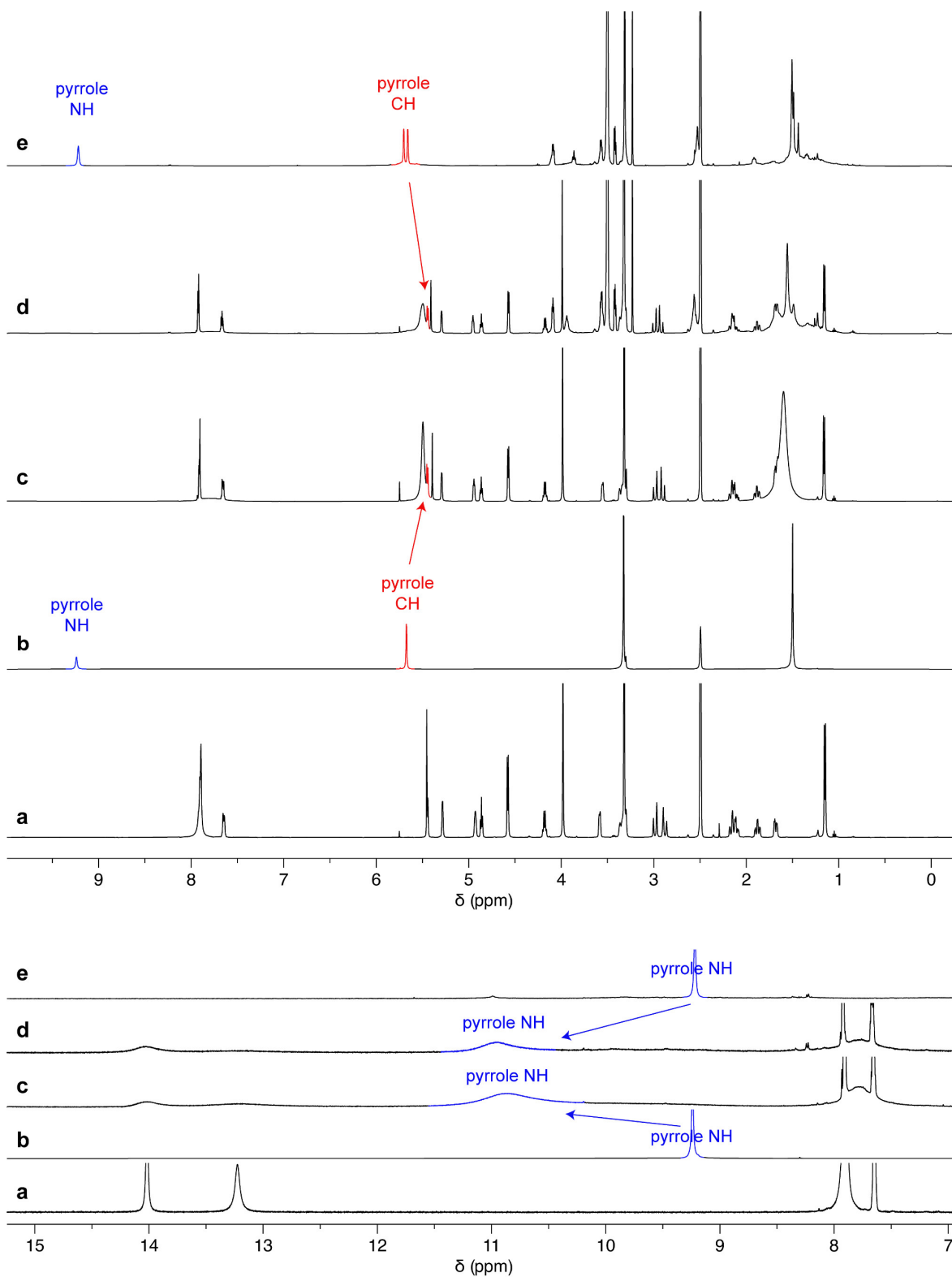
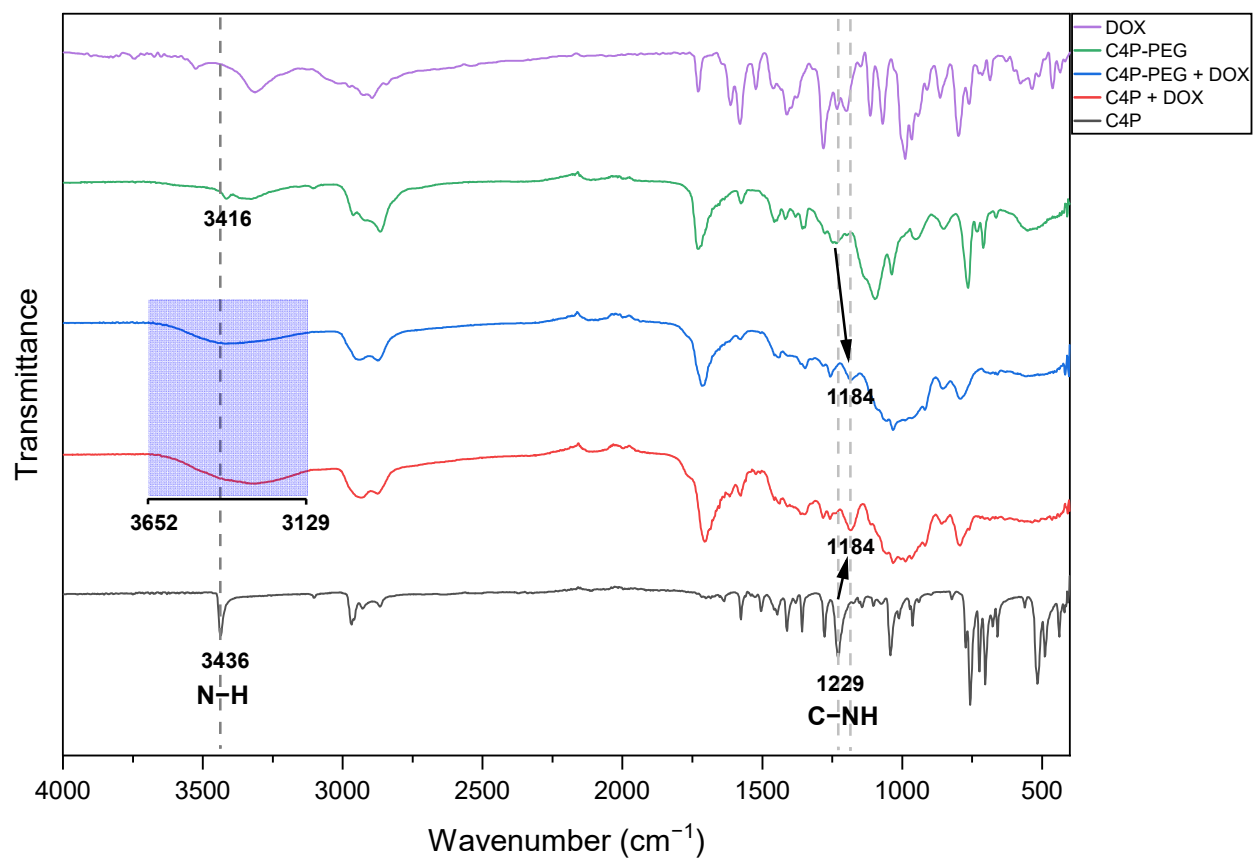


Fig S6. HR-ESIMS spectrum of C4P-PEG.



**Fig S7.** <sup>1</sup>H NMR spectra (500 MHz) of (a) DOX, (b) **C4P**, (c) **C4P + DOX**, (d) **C4P-PEG + DOX**, and (e) **C4P-PEG** recorded in DMSO-*d*<sub>6</sub>.

## FTIR Spectra



**Fig S8.** Stacked FTIR spectra of DOX, C4P, C4P+DOX, C4P-PEG, and C4P-PEG+DOX.

## UV-Vis Spectra

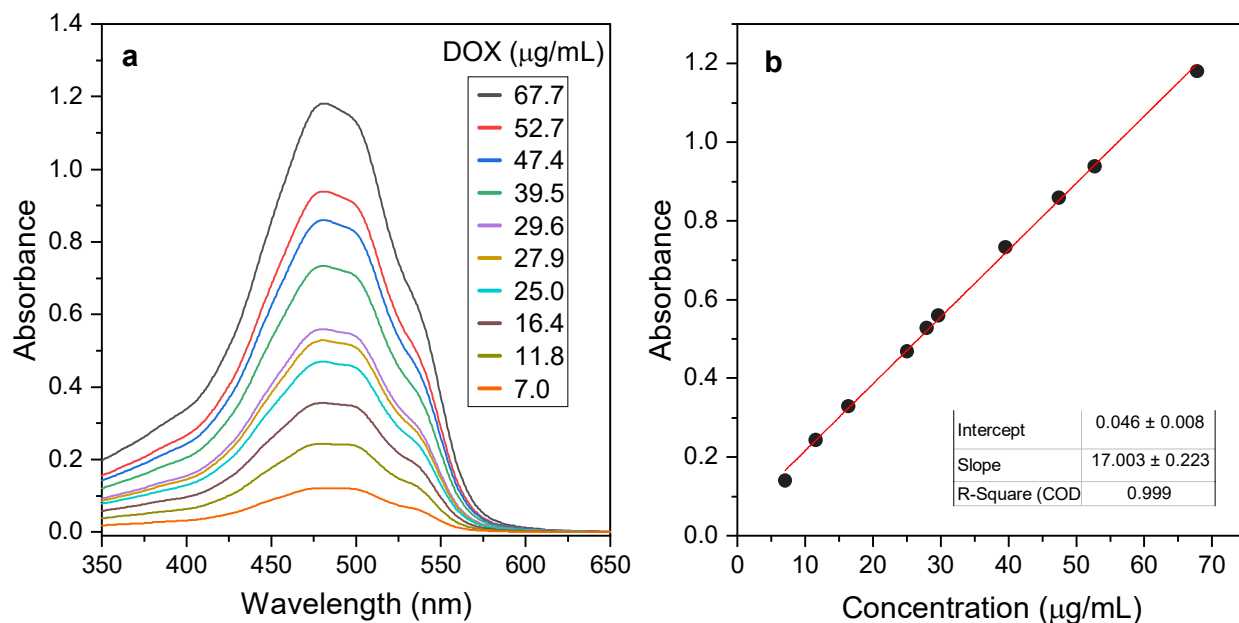


**Fig S9.** (a) UV-vis spectra of DOX in DMSO at varying concentrations and (b) the corresponding calibration curve generated from the absorbance values at 593 nm.

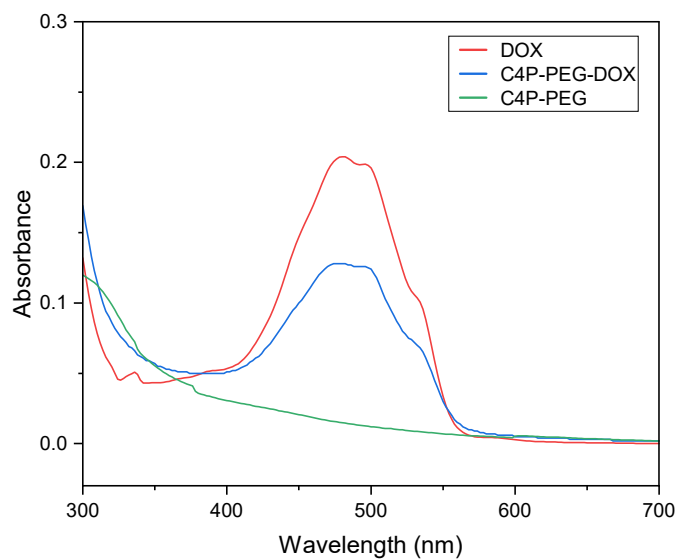


**Fig S10.** UV-vis spectra of **C4P-PEG**, DOX (before drug loading) and **C4P-PEG-DOX** (after drug loading).



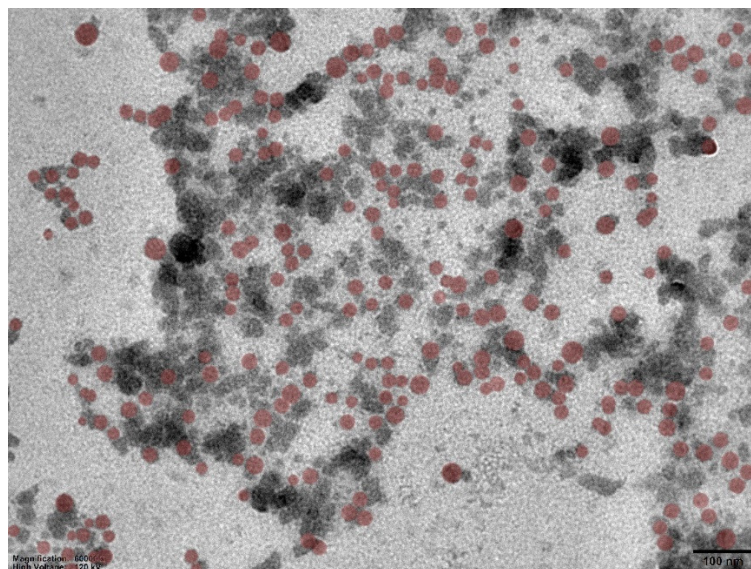


**Fig S11.** TEM image of **C4P-PEG** showing the selected aggregates (252 points) for the calculation of size distribution.

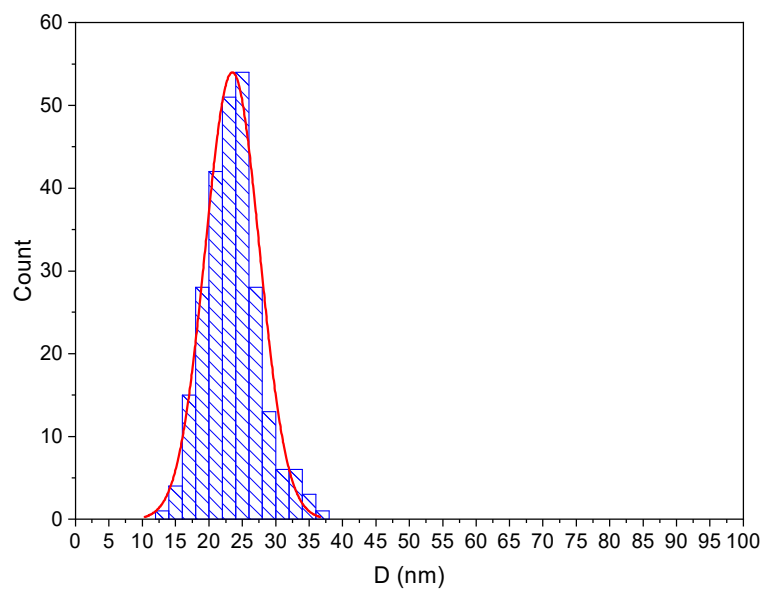


**Fig S12.** Size distribution of **C4P-PEG** based on the data obtained from Fig. S11.

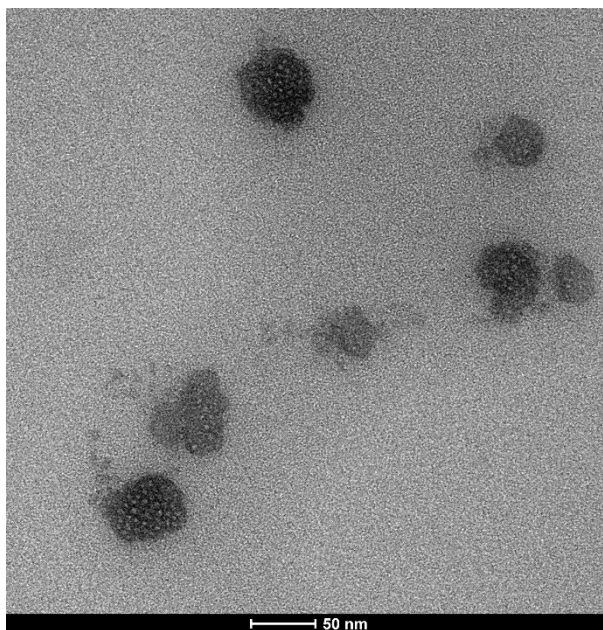


**Fig S13.** TEM image of **C4P-PEG-DOX**.

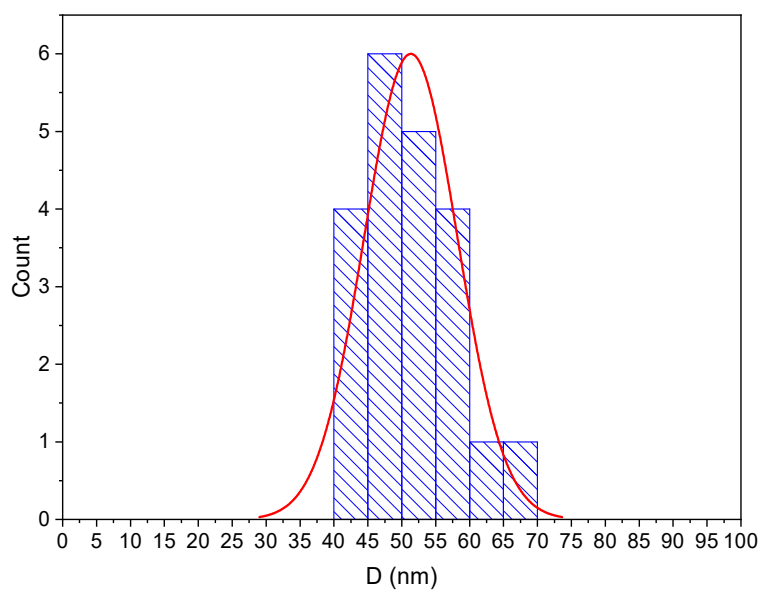


**Fig S14.** Size distribution of **C4P-PEG-DOX** based on the data obtained from Fig. S13.

## Binding Constant Determination and NOESY Analysis

To determine the stoichiometry and binding constant between calix[4]pyrrole core of **C4P-PEG** and DOX·HCl (through Cl<sup>-</sup> binding), <sup>1</sup>H NMR titrations were performed in DMSO-*d*<sub>6</sub> solutions which had a constant concentration of **C4P-PEG** (6.28 mM) and varying concentrations of DOX·HCl (Fig S16). By a non-linear curve-fitting method, the association constant between **C4P-PEG** and Cl<sup>-</sup> anion of DOX·HCl was determined to be  $1.55 \times 10^3 \pm 148 \text{ M}^{-1}$  by monitoring the pyrrole-CH protons of **C4P-PEG** (Fig. S15 and Fig. S16). The complexation stoichiometry was found to be 1:1 as shown in Fig. S17.

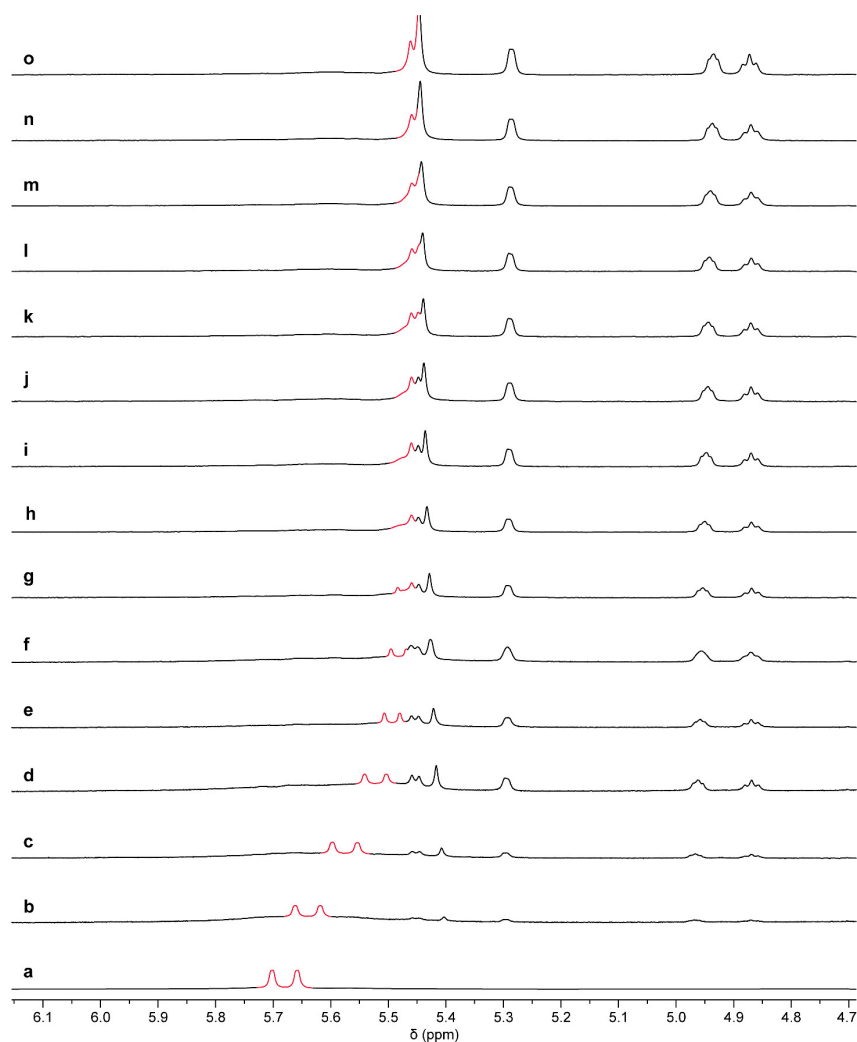
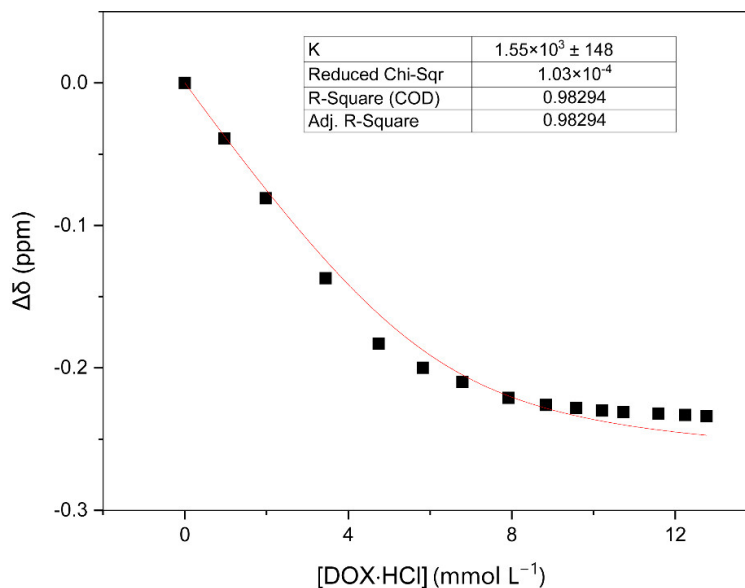


**Fig S15.** Partial <sup>1</sup>H NMR spectra (500 MHz, DMSO-*d*<sub>6</sub>, 25 °C) of **C4P-PEG** (6.28 mM) upon addition of DOX·HCl at 0.00, 0.98, 1.98, 3.45, 4.75, 5.82, 6.79, 7.92, 8.83, 9.58, 10.20, 10.74, 11.59, 12.24, 12.76 mM concentrations from bottom to top.



$$\Delta\delta = \Delta\delta_{max} \frac{[1 + K([H]_0 + [G])] - \sqrt{[1 + K([H]_0 + [G])]^2 - 4K^2[H]_0[G]}}{2K[H]_0}$$

**Fig S16.** Chemical shift changes of pyrrole CH protons (initially at 5.68 ppm) belonging to **C4P-PEG** (6.28 mM) upon incremental addition of DOX·HCl. The red solid line was obtained from a non-linear curve fitting using the equation provided under the figure.

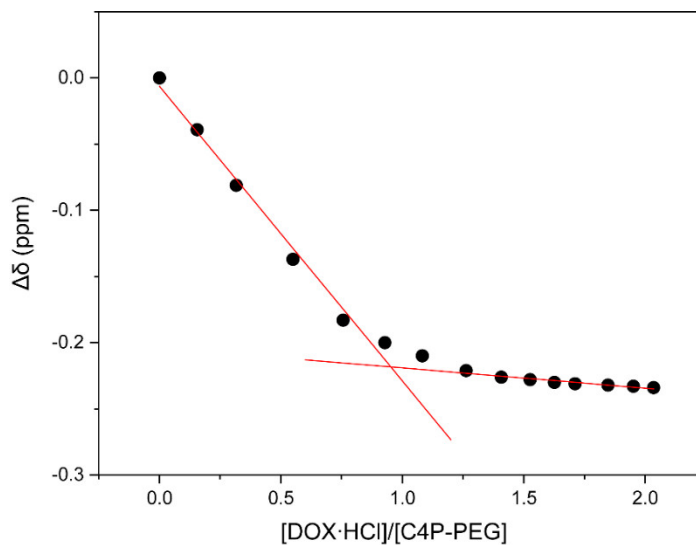


**Fig S17.** Molar ratio plot for the interaction of **C4P-PEG** with DOX·HCl, indicating a 1:1 stoichiometry.

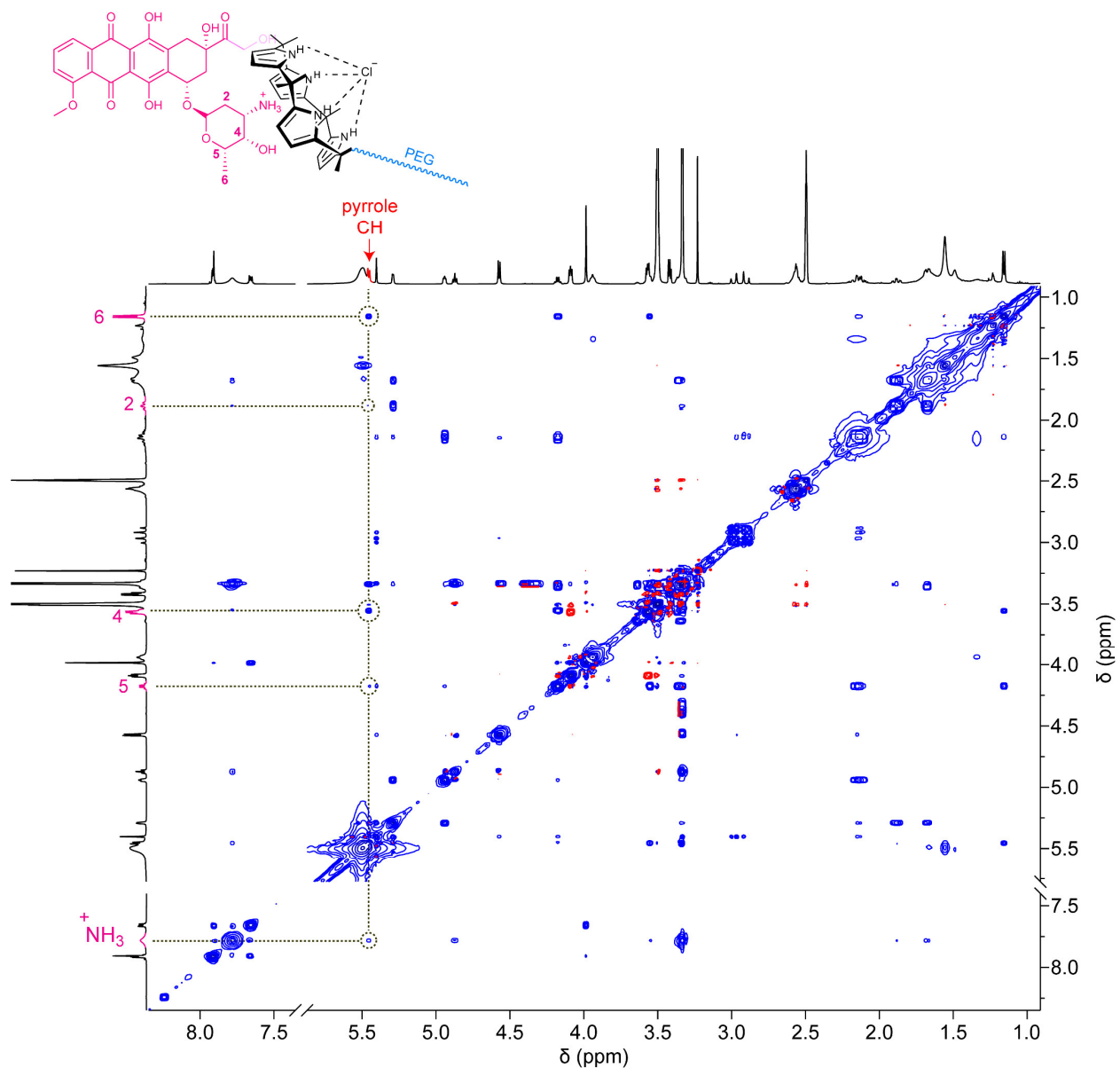


**Fig S18.** NOESY NMR spectrum of **C4P-PEG** + **DOX·HCl** (1:1) recorded in  $\text{DMSO-}d_6$  containing 1.5% (wt)  $\text{H}_2\text{O}$ . This spectrum shows the concurrent complexation of **C4P** core of **C4P-PEG** with  $-\text{NH}_3^+$  unit of **DOX·HCl** (see Fig S7 for peak shift changes in the case of  $\text{NH}\cdots\text{Cl}^-$  interaction) through cation- $\pi$  interaction.

## DLS and Zeta Potential Measurements

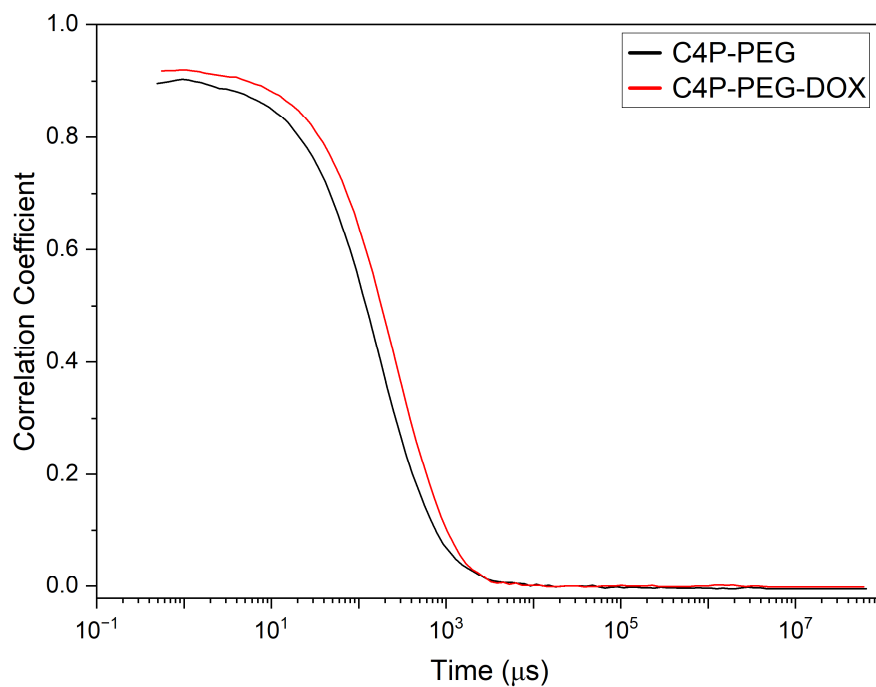


**Fig S19.** Correlation coefficient plots for **C4P-PEG** and **C4P-PEG-DOX** during DLS measurements.

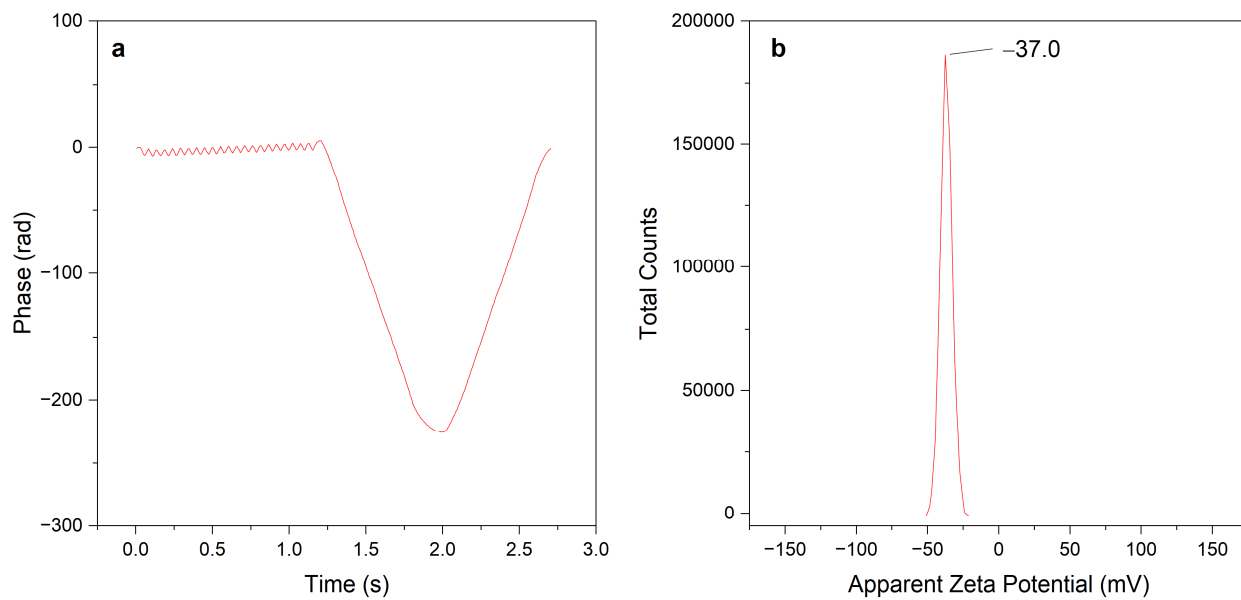


**Fig S20.** (a) Phase plot and (b) zeta potential distribution of **C4P-PEG**.

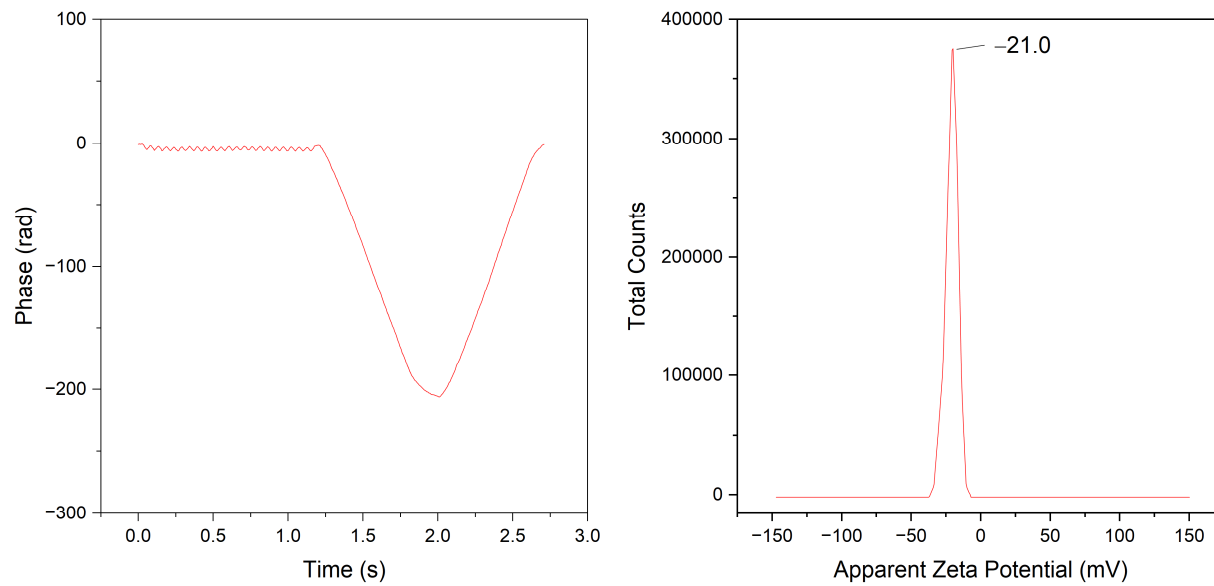


**Fig S21.** (a) Phase plot and (b) zeta potential distribution of **C4P-PEG-DOX**.

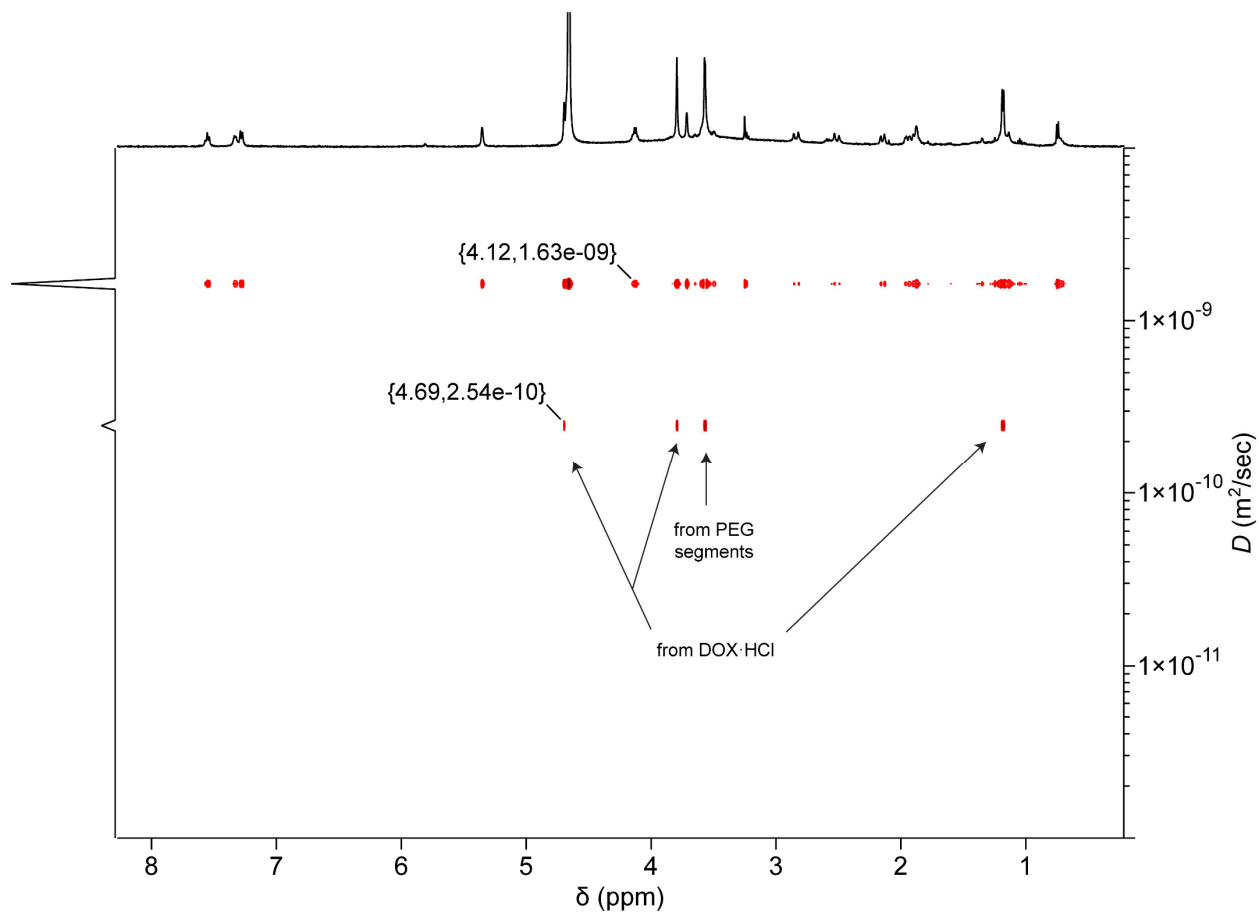


**Fig S22.** DOSY NMR spectrum of **C4P-PEG** + DOX·HCl (1:1) recorded in D<sub>2</sub>O (2.69 mM, 25 °C), showing the free (big trace) and encapsulated (small trace) DOX·HCl moieties.